

# Spin-polarized Dirac-Slater calculations on the energies of hollow argon atom

L. Natarajan<sup>a</sup>

Department of Physics, University of Mumbai, Mumbai 400098, India

Received 5 December 2000 and Received in final form 9 April 2001

**Abstract.** In this work, the multiplet splitting in terms of a spin-dependent model is analyzed. The spin-polarized and unpolarized single configuration Dirac-Fock-Slater wavefunctions have been used in the evaluation of the total energies of highly ionized argon with different L shell population. The transition energies of hollow argon atom with initial configurations  $1s_{1/2}^0 2s_{1/2}^m 2p_{1/2}^n 2p_{3/2}^l$  with  $m = 0$  to 2 and  $n + l$  varying from 6 to 1 are reported in this work. The calculations have been carried out by taking into account a relativistic exchange potential in the Dirac-Slater potential. To account for the correlation effects, a correction term has also been considered perturbatively. The present calculations show that the spin-polarized technique which is mainly applied to the ground states of atoms may also be applied to atoms ionized in the inner shells with a good degree of accuracy.

**PACS.** 32.80.Fb Photoionization of atoms and ions – 32.80.Dz Autoionization

## 1 Introduction

Electronic structure of atoms can be calculated by a variety of methods both in the framework of relativistic and non-relativistic theory. The one-particle Dirac-Fock-Slater model is one such relativistic approximation. In this method, the  $N$  electron wavefunctions are constructed from the one-electron Dirac-Fock atomic orbitals and the exchange potential is approximated by a local free electron gas expression. An exchange coefficient is incorporated in the exchange potential to minimize the total energy.

In the spin-polarized approximation, electrons with different spin projections (up or down) are considered as particles of two different states. It was first pointed out by Hartree [1] that the total energy of an atom in the Hartree-Fock model could be lowered by introducing spin polarization. This technique is successfully applied to neutral atoms with half filled outer shells, for a detailed description of the atomic level splitting [2] and in the study of photo-ionization cross-sections [3,4]. However, such calculations involving atoms ionized in the inner shells are not numerous. In this paper, an attempt has been made to extend such spin-polarized calculations to argon with a number of inner shell vacancies and open outer shells in order to study the influence of spin dependent charge density and potential on the total energies of the different atomic states [5]. Also, though argon is a light atom, relativistic effect plays an important role when it is highly ionized in the inner shells as the electrons now experience reduced screening.

In this paper, the total energies of a hollow argon atom [6,7] with different degrees of ionization in the  $n = 2$  shell

and all the electrons stripped out of the  $n = 3$  shell are calculated and the resulting K X-ray multiplet spectra are reported. Calculations have been carried out with initial configurations  $1s_{1/2}^0 2s_{1/2}^m 2p_{1/2}^n 2p_{3/2}^l$  using spin polarized and unpolarized one-electron Dirac-Slater wavefunctions. Here  $m$ ,  $n$  and  $l$  correspond to the occupation numbers of electrons in the  $2s_{1/2}$ ,  $2p_{1/2}$  and  $2p_{3/2}$  shells with  $m = 0$  to 2 and  $n + l = 6$  to 1. Recently Karim *et al.* [8] have carried out extensive calculations on the K X-ray and K-LL Auger hypersatellite spectra of hollow argon atoms with open outer shells and multiple inner shell vacancies using the multi-configuration Hartree-Fock atomic code developed by Cowan [9]. These calculations were performed using spin-unpolarized wavefunctions. The main purpose of the present work is to extend the relativistic spin-polarized technique to highly ionized argon and demonstrate that the spin-polarized scheme gives a proper description of multiplet splitting. The results from the present calculations are useful in the study of ion-surface and ion-cluster interactions.

## 2 Theory and procedure

The total energies of the argon atom ionized to different degrees are calculated in the spin-polarized approximation by setting up uncoupled Dirac-Slater equations using spin polarized atomic orbitals. Calculations have also been carried out using unpolarized Dirac-Fock-Slater wavefunctions.

It is well known that for a neutral atom with half-filled outer subshell, the interaction of the “up” electrons in the inner shells with the “up” electrons in the half-filled

---

<sup>a</sup> e-mail: lnn1@usa.net

outer shell is different from that of the “down” electrons and hence the ionization potential needed to remove an “up” electron from the atom is not the same as that for a “down” electron. This results in different energy splittings for a subshell with the same  $n$ ,  $l$  and  $j$  values but different spin (up or down) projections. In the same way, for a multiply ionized atom, the charge density from spin-up electrons need not be the same as that from spin-down electrons. As the wavefunction now is a function of spin projection also, the spin-polarized calculations would lead to different orbitals, different potentials and different eigenvalues for the two spin projections. The total charge density now becomes  $\rho = \rho^\uparrow + \rho^\downarrow$  where  $\rho^\uparrow$  and  $\rho^\downarrow$  are charge densities due to spin-up and spin-down electrons respectively. It should be pointed out here that in the spin-polarized treatment of atomic orbitals, the electron spin is not a good quantum number. However this does not give rise to any significant error in the energy calculations [10].

In the Dirac-Fock method, the different atomic orbitals are given by the four-component solutions of the Dirac equation while the Coulomb interaction is the same as in the Hartree-Fock model. A correction term of the order of  $\alpha^2$  where  $\alpha$  is the fine structure constant has been incorporated perturbatively [11–13] in the non-relativistic Hartree-Fock potential to account for the relativistic effect. In the Dirac-Slater method, the direct terms of the electron-electron potential energy are computed as in the Dirac-Fock method but the exchange terms are approximated by a local potential determined from the statistical free electron gas with the spherically averaged charge or spin density of electrons as independent variable [14]. In the Dirac-Kohn-Sham method, the exchange coefficient is adjusted to give a minimum value for the total energy.

The one-particle Dirac-Slater equation in atomic units is

$$[c\hat{\alpha}\hat{p} + (\beta - 1)c^2 + V_{\text{eff}}(\hat{r})]\Psi_{i,\sigma} = \varepsilon_{i,\sigma}\Psi_{i,\sigma} \quad (1)$$

where  $\alpha$  and  $\beta$  are the usual Dirac matrices and  $V_{\text{eff}}$  is the effective potential comprising of the classical Coulomb electron-nuclear interaction, electron-electron interaction, exchange interaction and correlation effects. Here  $\sigma$  is the spin index and  $\Psi_{i,\sigma}$  are the four component spinors. The rest energy  $c^2$  has been subtracted out.

In terms of  $\Psi_{i,\sigma}$ , the total electron density can be expressed as

$$\rho = \sum_{\sigma} \sum_{i=1}^{N_{\sigma}} \Psi_{i,\sigma}^{\dagger}(\vec{r})\Psi_{i,\sigma}(\vec{r}) = \sum_{\sigma} \sum_{i=1}^{N_{\sigma}} \rho_{i,\sigma}(\vec{r}). \quad (2)$$

The average exchange energy per electron is

$$\varepsilon_x(\rho) = -\frac{3(3\pi^2\rho)^{1/3}}{4\pi} \quad (3)$$

and the non-relativistic exchange potential taking into account the Kohn-Sham exchange coefficient  $\alpha$  is then

given by

$$\begin{aligned} V_{\text{ex}}^{\text{NR}} &= \frac{\delta E_{\text{ex}}(\rho)}{\delta\rho(\vec{r})} \\ &= \frac{\delta}{\delta\rho(\vec{r})} \left[ \int \rho(\vec{r})\varepsilon_x(\rho)d\vec{r} \right] = -3\alpha \left( \frac{3\rho}{4\pi} \right)^{1/3}. \end{aligned} \quad (4)$$

Neglecting self-correlation energy, the incremental correlation energy per electron  $\varepsilon_c(r_s)$  obtained by adding one electron at a time can be expressed as [9]

$$\varepsilon_c(r_s) = -\frac{1}{2} \left[ 4(r_s + 9)^{1/2} + \frac{3}{4}(1.142r_s) \right]^{-1} \quad (5)$$

where  $r_s$  is the radius of a sphere whose volume is the average volume per electron.

The relativistic correction to the exchange potential in the Dirac-Slater equation was developed by Ellis [15]. The unpolarized relativistic exchange potential in the Dirac-Kohn-Sham-Slater model can be expressed approximately as

$$V_{\text{ex}}^{\text{rel}} = -3(3\rho/4\pi)^{1/3} \left( 1 - \frac{\lambda}{9} - \frac{7\lambda^2}{180} \right) \quad (6)$$

where

$$\lambda = k^2 / (k^2 + c^2). \quad (7)$$

The Fermi momentum

$$k = (6\pi^2\rho)^{1/3} \quad \text{and} \quad c = 1/\alpha. \quad (8)$$

As the contribution from the correlation energy is small, the correlation potential is added as a small correction term at the end of the calculation.

In our evaluation of local spin densities, the contribution from the small components has also been taken into account. The initial configurations considered in this work in the spin-polarized Dirac-Slater method are of the form  $1s^0 2s^0 2p_{1/2}^n 2p_{3/2}^l$ ,  $1s^0 2s^1(\uparrow) 2p_{1/2}^n 2p_{3/2}^l$ ,  $1s^0 2s^1(\downarrow) 2p_{1/2}^n 2p_{3/2}^l$  and  $1s^0 2s^2 2p_{1/2}^n 2p_{3/2}^l$  with  $n = 0$  to 2 and  $l = 0$  to 4. The calculations have been carried out in the LS coupling approximation assuming a point nucleus. Though the 1s electron in the final state can have either a spin-up or spin-down projection, in this work the 1s electron is assumed to be occupying the spin-up state. In the spin-unpolarized Dirac-Slater method, the initial configurations considered are  $1s^0 2s^m 2p_{1/2}^n 2p_{3/2}^l$  with  $m$  and  $n$  varying from 0 to 2 and  $l$  from 0 to 4.

### 3 Results and discussion

The total energies of the various initial and final configurations of argon with different degrees of ionization in the L shell were calculated using spin-polarized and spin-unpolarized Dirac-Slater wavefunctions. The energies of the K X-ray photons originating from states with initial

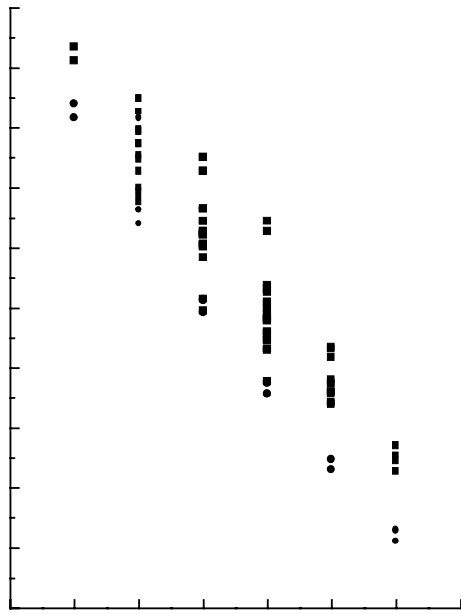


**Fig. 1.** Spin-polarized (squares) and unpolarized (circles) K X-ray energies of argon originating from the initial configurations  $2p_{1/2}^n 2p_{3/2}^l$  with  $n+l = 6$  to 1 as a function of number of  $2p$  electrons.

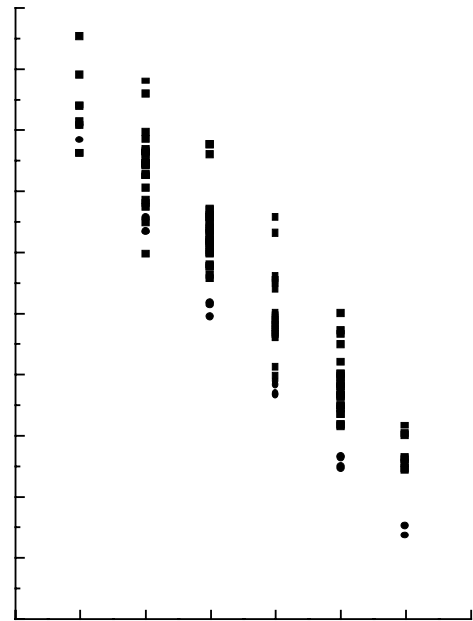


**Fig. 2.** Spin-polarized (squares) and unpolarized (circles) K X-ray energies of argon originating from the initial configurations  $2s_{1/2} 2p_{1/2}^n 2p_{3/2}^l$  with  $n+l = 6$  to 1 as a function of number of  $2p$  electrons.

configurations  $1s^0 2s^1(\uparrow) 2p_{1/2}^n 2p_{3/2}^l$ ,  $1s^0 2s^1(\downarrow) 2p_{1/2}^n 2p_{3/2}^l$  and  $1s^0 2s^2 2p_{1/2}^n 2p_{3/2}^l$  with  $n+l = 6$  to 1 are plotted as a function of number of  $2p$  electrons in Figures 1 to 3 respectively. Also included in these figures are the unpolarized Dirac-Slater energies. Each figure corresponding to a particular value of  $m$  ( $m = 0, 1$  and  $2$ ) where  $m$  is the number of spectator electrons in the  $2s$  subshell can be divided into six groups of transitions, each group corresponding to a specific value of  $n+l$ . It is seen from Figures 1 and 3 that the K X-rays have distinct energy values only when  $n+l$  is either 6 or 1. For other values of  $n+l$ , the figures show a number of closely spaced lines forming small groups. The transition energies plotted in Figure 2 do not exhibit a well-separated structure for any value of  $n+l$ . A comparison of the three figures shows that there are some transitions with different values of  $m+n+l$ , giving rise to overlapping lines.

For the same  $m$ , for which the value of  $n+l$  decreases from 6 to 1, the energy of the X-ray photon increases gradually as the spectator electrons in the L shell now experience a lesser screening effect. Similarly, for the same  $n+l$  value but different  $m$  ( $m = 0-2$ ), the energy of the photon decreases with increasing value of  $m$ . The systematic variations in the energies of X-rays with the number of electrons in the L shell and the complexity of the multiplet structure are evident from these figures. There is more clustering of lines in Figure 2 than in Figures 1 and 3.

The energy of the emitted radiation depends on the spin projections of the electrons occupying the initial and final states. Among the various possible transitions that can be conceived of for a given number of spectator

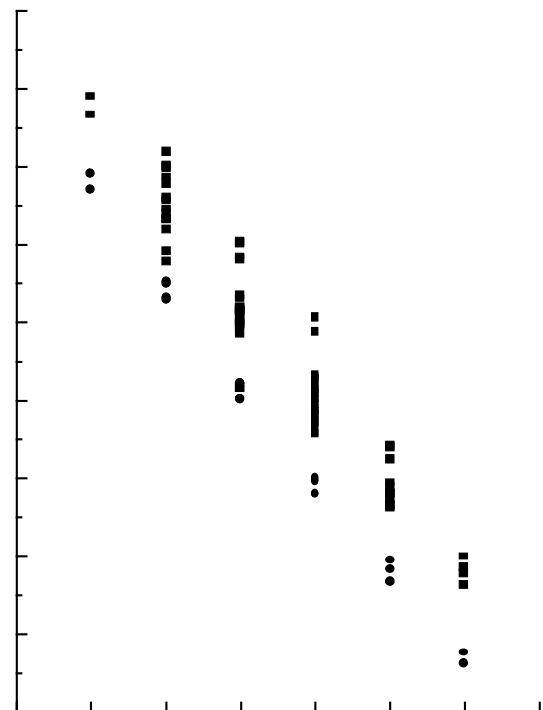


**Fig. 3.** Spin-polarized (squares) and unpolarized (circles) K X-ray energies of argon originating from the initial configurations  $2s_{1/2}^2 2p_{1/2}^n 2p_{3/2}^l$  with  $n+l = 6$  to 1 as a function of number of  $2p$  electrons.

electrons in the L shell, it is found that in general the energy of the photon shoots up to a high value when the electrons in the initial configuration are in the spin-up states with only one electron in the spin-down state and the electrons in the final state have only spin-up projections. The transition energy falls to a low value when these electrons occupy the spin-down initial states with one electron in the spin-up state and during the transition, the spin-up electron goes to the empty  $1s$  shell. Apart from these two extreme cases, the rest of the K X-rays with a particular value of  $m + n + l$  give rise to closely spaced lines.

The unpolarized Dirac-Slater calculations reported in this work indicate that as the number of spectator electrons in the  $2s$  subshell decrease by one, the energies of the X-ray photons originating from the same initial configurations corresponding to a certain value of  $n + l$  differ on an average by 20 to 25 eV. For a given  $m$ , as the number of electrons initially in the  $2p$  shell decrease by one the increase in the energies of the K X-rays range from 20 to 30 eV giving rise to a distinct spectra. A comparison of single configuration spin-polarized and unpolarized Dirac-Slater energies show that the energy range of K X-rays in the spin polarized treatment is in general more than the unpolarized values by approximately 15 to 40 eV. The present calculations show that the spin-polarized effects are large in lowering the total energies of the final states and the difference between the polarized and unpolarized total energy ranges from 25 to 45 eV. However the difference is, in general, marginal for the initial states.

As the aim of the present work is to determine the accuracy of spin-polarized and unpolarized techniques in the energy evaluation of the excited states, the median energy values of the photons listed in this paper are compared with the MCHF median energy values of the K X-rays reported by Karim *et al.* [8]. Their MCHF median energy values of the K X-rays originating from the initial configurations  $1s^0 2s^0 2p^n$  are 3186, 3212, 3237, 3263 and 3293 eV respectively for  $n = 6, 5, 4, 3$  and  $2$  and the median energies of the photons arising due to the decay of the configuration  $1s^0 2s^0 2p_{1/2}^n 2p_{3/2}^l$  calculated using spin-polarized approach are 3170, 3195, 3218, 3247, 3274 and 3305 eV for  $n + l = 6$  to  $1$  respectively. A comparison shows that the energies of the K X-rays calculated using the spin-polarized scheme are less than the MCHF values by 16 eV whereas the unpolarized calculations are nearly 35 to 40 eV less than the MCHF median energy values. Similar variations are also found in the median energy values of the X-rays arising from the other two initial configurations.

As the spin-up and spin-down charge densities of the spectator electrons in the various initial and final states considered in this work are not the same, the exchange potentials will also be different depending on the charge densities. For example, the variation of the spin-up and spin-down relativistic exchange potentials for the final configuration  $1s^1(\uparrow)2s^2 2p_{1/2}^1(\downarrow)2p_{3/2}^1(\uparrow)$  and initial configurations  $1s^0 2s^2 2p_{1/2}^1(\downarrow)2p_{3/2}^2(\uparrow\downarrow)$ ,  $1s^0 2s^2 2p_{1/2}^1(\downarrow)2p_{3/2}^2(\uparrow\uparrow)$  and  $1s^0 2s^2 2p_{1/2}^1(\downarrow)2p_{3/2}^2(\downarrow\downarrow)$  with the radial distance are drawn in Figures 4, 5, 6 and 7 respectively. In Figure 4, the spin-up and spin-down

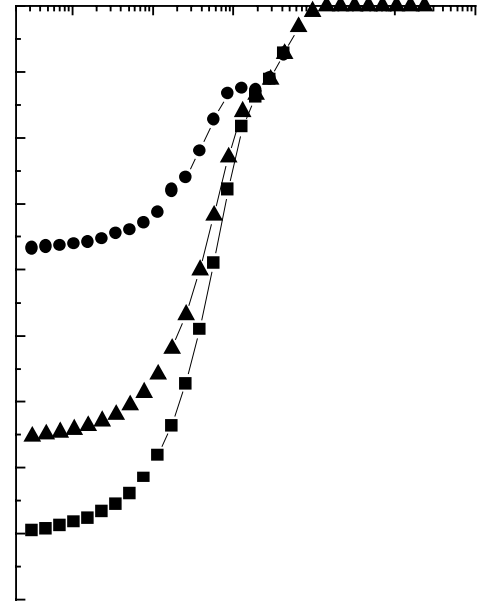


**Fig. 4.** Relativistic Dirac-Slater exchange potentials  $V_{\text{ex}}(r)$  in a.u. in the spin-polarized and unpolarized schemes for the final configuration  $1s^1(\uparrow)2s^2 2p_{1/2}^1(\downarrow)2p_{3/2}^1(\uparrow)$  as a function of  $\log r$ . Squares: spin-up potential, circles: spin-down potential, triangles: unpolarized potential.

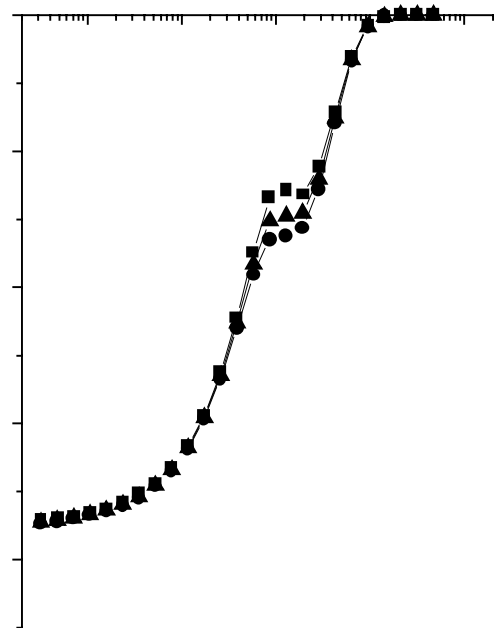


**Fig. 5.** Relativistic Dirac-Slater exchange potentials  $V_{\text{ex}}(r)$  in a.u. in the spin-polarized and unpolarized schemes for the initial configuration  $1s^0 2s^2 2p_{1/2}^1(\downarrow)2p_{3/2}^2(\uparrow\downarrow)$ , as a function of  $\log r$ . See Figure 4 for symbol illustrations.

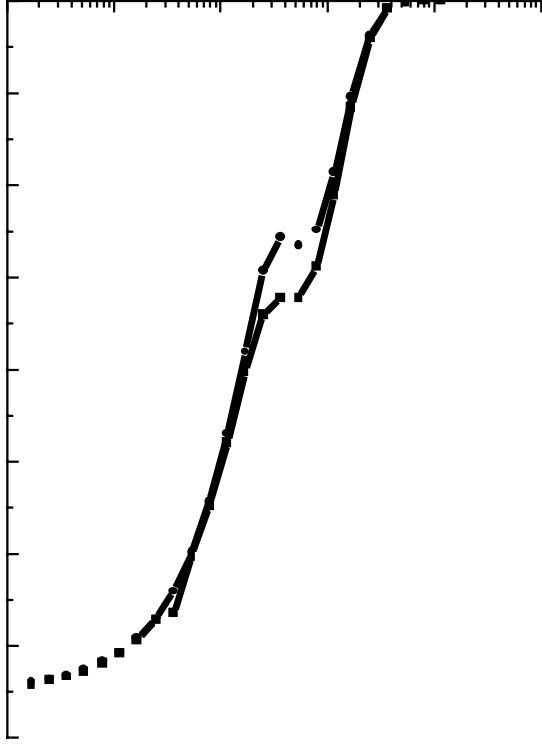


**Fig. 6.** Relativistic Dirac-Slater spin-polarized exchange potential  $V_{\text{ex}}(r)$  in a.u. for the initial configuration  $1s^0 2s^2 2p_{1/2}^1(\downarrow) 2p_{3/2}^2(\uparrow\uparrow)$  as a function of  $\log r$ . See Figure 4 for symbol illustrations.

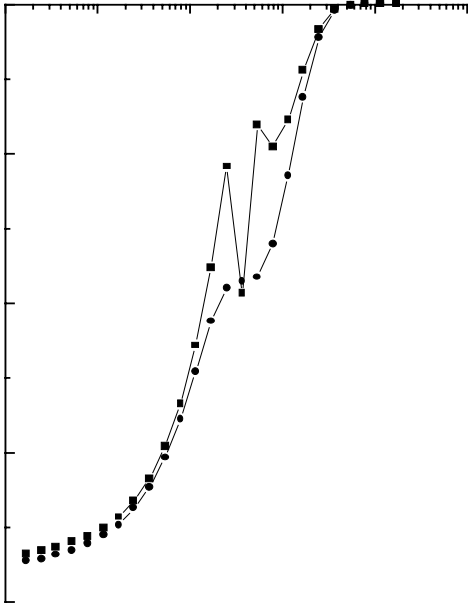


**Fig. 7.** Relativistic Dirac-Slater spin-polarized exchange potential  $V_{\text{ex}}(r)$  in a.u. for the initial configuration  $1s^0 2s^2 2p_{1/2}^1(\downarrow) 2p_{3/2}^2(\downarrow\downarrow)$  as a function of  $\log r$ . See Figure 4 for symbol illustrations.

relativistic exchange potentials for the final configuration  $1s^1(\uparrow) 2s^2 2p_{1/2}^1(\downarrow) 2p_{3/2}^1(\uparrow)$  as a function of  $\log r$  where  $r$  is the radial distance, are plotted. Also included in this figure is the unpolarized exchange potential for the final configuration  $1s^1 2s^2 2p_{1/2}^1 2p_{3/2}^1$ . As the spin-up electron in the  $1s$  shell is close to the nucleus, its influence on the spin-up potential is more than that of spin-down potential for small values of  $r$  as is evident from the figure. As the value of  $r$  increases, the difference in the exchange potentials decreases and the spin-up and spin-down potentials are nearly the same for values of  $r$  beyond 0.3 a.u. At a radial distance of the order of 0.13 a.u. the spin-down potential gives rise to a glitch whose origin is not clear. It is seen from the figure that the unpolarized potential is less negative than the spin-up potential, but more attractive than the spin-down potential.

In Figures 5, 6 and 7 are plotted the spin-up and spin-down relativistic exchange potentials for the three possible spin projections of the two electrons in the  $2p_{3/2}$  subshell with configurations  $1s^0 2s^2 2p_{1/2}^1(\downarrow) 2p_{3/2}^2(\uparrow\downarrow)$ ,  $1s^0 2s^2 2p_{1/2}^1(\downarrow) 2p_{3/2}^2(\uparrow\uparrow)$  and  $1s^0 2s^2 2p_{1/2}^1(\downarrow) 2p_{3/2}^2(\downarrow\downarrow)$  respectively as a function of  $\log r$ . Also included in Figure 5 is the unpolarized exchange potential for the initial configuration  $1s^0 2s^2 2p_{1/2}^1 2p_{3/2}^2$ . It is seen from these figures that the spin-up and spin-down potentials are the same for very small and very large values of  $r$ . However for  $r \sim 0.15$  a.u., the spin-up exchange potential differs from spin-down potential and its value is either larger or smaller than that of spin-down potential depending upon its charge density. Also seen in these three figures are glitches both in the spin-up and spin-down potentials at  $r \sim 0.13$  a.u. in Figure 5 and  $r \sim 0.16$  a.u. in Figures 6 and 7. However, when the spin-up and spin-down charge densities of electrons in a given configuration are the same (for example configurations like  $1s^0 2s^2 2p_{1/2}^1(\downarrow) 2p_{3/2}^1(\uparrow)$  and  $1s^2 2s^2 2p_{1/2}^1(\downarrow) 2p_{3/2}^1(\uparrow)$ ), the glitches are absent in the exchange potentials. The unpolarized potential coincides with the spin-up and spin-down potentials both for the smaller and larger values of  $r$  and the glitch is observed in this case as well.

## 4 Conclusion

This work attempts to illustrate the applicability and accuracy of the relativistic spin-polarized  $X_\alpha$  method in energy calculations of highly ionized atom. The present calculations show that the spin-dependent scheme gives a proper description of multiplet splitting with a good degree of accuracy. It is found that the relativistic corrections to the potential due to spin-up and spin-down charge densities do play an important role when the atom is ionized to different degrees in the inner and outer shells. The results of this work could provide valuable information on the spin projections of electrons involved in different transitions found from analyzing the experimental spectra of highly ionized argon.

The author gratefully acknowledges the financial support by BRNS, Department of Atomic Energy, India for carrying out this work.

## References

1. D.R. Hartree, Rep. Progr. Phys. **11**, 113 (1947).
2. J.C. Slater, *The self-consistent field for molecules and solids* (McGraw-Hill, New York, 1974).
3. M.Ya. Amusia, V.K. Ivanov, L.V. Chernysheva, J. Phys. B At. Mol. Phys. **34**, L19 (1981).
4. V.K. Ivanov, L.V. Chernysheva, Opt. Spectrosc. **69**, 289 (1990).
5. L. Natarajan, *18th Int. Conf. on X-ray and Inner shell processes*, edited by D.S. Gemmel, G.K. Shenoy, Illinois, Book of Abstracts, p. 265 (1999).
6. J.P. Briand, L. de Billy, P. Charles, E. Essabaa, P. Briand, R. Geller, J.P. Desclaux, S. Bliman, C. Ristori, Phys. Rev. Lett. **65**, 159 (1990).
7. J.P. Briand, Comm. At. Mol. Phys. **33**, 1 (1996).
8. K.R. Karim, S.R. Grabbe, C.P. Bhalla, J. Phys. B At. Mol. Phys. **29**, 4007 (1996).
9. R.D. Cowan, *The Theory of Atomic Structure and Spectra* (University of California Press, 1981).
10. G.F. Gribakin, A.A. Gribakina, B.V. Gultsev, V.K. Ivanov, J. Phys. B At. Mol. Phys. **25**, 1757 (1992).
11. I.P. Grant, Adv. Phys. **19**, 747 (1970).
12. J.B. Mann, W.R. Johnson, Phys. Rev. A **4**, 41 (1971).
13. J.P. Desclaux, Comput. Phys. Commun. **9**, 31 (1975).
14. A. Rosen, I. Lindgren, Phys. Scripta **6**, 109 (1972).
15. D.E. Ellis, J. Phys. B At. Mol. Phys. **10**, 1 (1977).